

Saturating the one-axis twisting quantum Cramér-Rao bound with a total spin readout

T.J. Volkoff

Theoretical Division, Los Alamos National Laboratory, Los Alamos, NM, USA.

Michael J. Martin

Materials Physics and Applications Division, Los Alamos National Laboratory, Los Alamos, NM, USA.

We show that the lowest quantum Cramér-Rao bound achievable in interferometry with a one-axis twisted spin coherent state is saturated by the asymptotic method-of-moments error of a protocol that uses one call to the one-axis twisting, one call to time-reversed one-axis twisting, and a final total spin measurement (i.e., a twist-untwist protocol). The result is derived by first showing that the metrological phase diagram for one-axis twisting is asymptotically characterized by a single quantum Fisher information value $N(N+1)/2$ for all times, then constructing a twist-untwist protocol having a method-of-moments error that saturates this value. The case of finite-range one-axis twisting is similarly analyzed, and a simple functional form for the metrological phase diagram is found in both the short-range and long-range interaction regimes. Numerical evidence suggests that the finite-range analogues of twist-untwist protocols can exhibit a method-of-moments error that asymptotically saturates the lowest quantum Cramér-Rao bound achievable in interferometry with finite-range one-axis twisted spin coherent states for all interaction times.

I. INTRODUCTION

The quantum Cramér-Rao inequality (QCRI) implies that interacting quantum spin systems allow to estimate SU(2) rotations with quadratically lower error (in the system size) than is achievable with classical spins. For a given rotation defining the quantum estimation problem, construction of a protocol that approximately saturates the QCRI subject to dynamical and kinematical constraints of the quantum spin system is a central part of quantum metrology research in atomic systems. A generic noiseless protocol can be constructed as

$$|\psi\rangle \rightarrow U|\psi\rangle \rightarrow R_\phi U|\psi\rangle \rightarrow V R_\phi U|\psi\rangle \rightarrow f(\phi) \quad (1)$$

where the steps correspond to 1. pre-rotation evolutions of the probe quantum system, 2. rotation, 3. post-rotation evolution of the probe, 4. measurement of a linear or nonlinear signal $f(\phi)$ from which to extract the rotation estimate. The signal depends on $|\psi\rangle$, U , V , and the chosen quantum measurement. In (1), the restriction to pure probe states and unitary evolutions is due to the fact that noisy quantum states never provide the greatest quantum Fisher information (QFI) defining the lowest lower bound in the QCRI for the error of a rotation estimation protocol.

Protocols that take U and V to be one-axis twisting evolutions [1] or finite-range one-axis twisting evolutions have proven central to high-performance quantum rotation estimation protocols [2–6]. There are two physical reasons for this: 1. one-axis twisting generates spin squeezing, 2. one-axis twisting naturally appears as the effective interaction in low-energy, two-mode atomic systems. In fact, for interaction time $\pi/2$, one-axis twisting generates a Greenberger-Horne-Zeilinger (GHZ) state with direction dependent on the parity of N . Such a GHZ state allows to achieve the global Heisenberg limit

for sensing an SU(2) rotation (global Heisenberg limit refers to the quantum Fisher information being equal to N^2 for all ϕ). To see this, consider the GHZ probe state evolving under a differential phase shift according to

$$|\psi_\phi\rangle := e^{-i\phi J_z} \frac{|N, 0\rangle + |0, N\rangle}{\sqrt{2}} \quad (2)$$

[7]. When using a global measurement of X to estimate ϕ , the method of moments estimator $\hat{\theta}$ [8] of the rotation angle θ has normal distribution with variance given by

$$\begin{aligned} (\Delta\tilde{\phi})^2 &:= \frac{\text{Var}_{|\psi_\phi\rangle} X^{\otimes N}}{(\partial_\phi \langle X^{\otimes N} \rangle_{|\psi_\phi\rangle})^2} \\ &= \frac{1 - \langle X^{\otimes N} \rangle_{|\psi_\phi\rangle}^2}{(\partial_\phi \langle X^{\otimes N} \rangle_{|\psi_\phi\rangle})^2} \\ &= \frac{1}{N^2} \end{aligned} \quad (3)$$

for all ϕ . Although the above example protocol has no faults in a digital quantum device that utilizes, e.g., a Hadamard and CNOT circuit to generate the GHZ state and carries out measurement of an N -qubit Pauli group observable, the example may be infeasible in an analog quantum system such as an atomic gas, in which a linear depth circuit involving pairwise-entangling gates and measurements of the individual particles cannot be implemented due to a lack of addressability. One could note that the same method-of-moments sensitivity can be obtained by measuring the symmetric operator $|N, 0\rangle \langle 0, N| + h.c.$ [9], which does not require a measurement to be carried out on individual atoms. This is true, but if the measurement statistics of this operator are to be obtained by counting the occurrences of $|N, 0\rangle$ and $|0, N\rangle$ by number difference measurement, a GHZ-generating circuit must still appear somewhere in the

protocol to convert the eigenvectors of $|N, 0\rangle \langle 0, N| + h.c.$ to those of $|N, 0\rangle \langle N, 0| + |0, N\rangle \langle 0, N|$.

The problem of generating the GHZ state in an analog system is usually solved by appealing to spin-squeezing entanglement generation. By the Yurke-Stoler process, one finds that, for even N , one-axis twisting dynamics $e^{-itJ_z^2}$ generates a GHZ state in a given direction on the Bloch sphere from a spin coherent state in that direction for $t = \pi/2$. For odd N , the resulting GHZ state is rotated by $\pi/2$ relative to the initial axis. The quality of the GHZ state depends on whether the interaction time $t = \pi/2$ can be reached with high state fidelity. However, the problem of finding an alternative measurement scheme remains. One class of methods to resolve this problem involves applying a second one-axis twisting operation to create the probe state $e^{it_2J_z^2}$, and replacing the global measurement $X^{\otimes N}$ by a measurement of a total spin operator $\vec{n} \cdot \vec{J}$ to yield an estimate of the probability distribution $p_m(\phi)$, $m = \{-\frac{N}{2}, -\frac{N}{2} + 1, \dots, \frac{N}{2}\}$ [10]. In this case, the ϕ signal is the probability density corresponding to a total spin measurement.

On the other hand, in practice it is desirable to design metrology protocols that obtain a parameter estimate from the minimal possible information obtainable from a measurement, e.g., that use low moments of a total spin operator as the ϕ signal. For instance, it has been noted that Heisenberg scaling can be attained by carrying out total spin measurement on a probe state prepared by two calls to one-axis twisting dynamics (with small interaction times $t \sim \frac{1}{\sqrt{N}}$) [2]. Specifically, this probe state is prepared by twist-untwist protocol, which we define as

$$|\psi_\phi(\vec{n})\rangle = e^{itJ_z^2} e^{-i\phi\vec{n}\cdot\vec{J}} e^{-itJ_z^2} |\zeta = 1\rangle, \quad (4)$$

and an estimate of ϕ is obtained by measurement of the total spin operator $\vec{m} \cdot \vec{J}$. In (4), we use the SU(2) coherent state

$$|\zeta\rangle = \frac{1}{(1 + |\zeta|^2)^{N/2}} \sum_{\ell=0}^N \sqrt{\binom{N}{\ell}} \zeta^\ell |N - \ell, \ell\rangle \quad (5)$$

where $|N - \ell, \ell\rangle$ is the Dicke state (i.e., number occupation basis state) with ℓ particles in $|1\rangle$, and $\zeta \in \mathbb{C} \cup \{\infty\}$ is the stereographic projection from the south pole of the Bloch sphere). Also in (4), the dependence of the state on N and t has been suppressed in the notation of the right hand side. In [6], the untwist layer of the protocol. In this work, we show analytically that the method-of-moments error of an optimal twist-untwist protocol saturates the QCRB for the one-axis twisting path $e^{-itJ_z^2} |\zeta = 1\rangle$ asymptotically for all interaction times. We provide numerical evidence for the same statement when one-axis twisting generator J_z^2 is replaced by a finite-range one-axis twisting generator with K spin interactions [11]. These results show that twist-untwist protocols, which utilize a total spin readout but require control of the sign of atomic interactions, are metrologically equivalent to a protocol that performs optimal

quantum estimation of the rotation angle of a one-axis twisted probe state about its most sensitive axis.

Section II provides background on the asymptotic (in the number of measurement shots) method-of-moments error that is used to quantify the sensitivity of twist-untwist protocols in this manuscript, and shows how, when combined with a twist-untwist protocol and total spin measurement, this error achieves the Heisenberg limit globally over all rotation angles. Section III derives a metrological phase diagram for one-axis twisting building on previous work analyzing the asymptotics of QFI and spin squeezing in this system [12–15]. It is also shown that for large N , a QFI plateau with value $N(N+1)/2$ is for all interaction times except a set of asymptotic measure zero. Section IV identifies a twist-untwist protocol and total spin measurement with method-of-moments error that asymptotically saturates the maximal QFI for a one-axis twisted probe state on this plateau. Section V derives a metrological phase diagram for finite-range one-axis twisting for both cases of short-range and long-range interactions, with subsection V A providing numerical evidence that a twist-untwist protocol and total spin measurement saturates the maximal QFI for a finite-range one-axis twisted probe state, at least for a large range of interaction times.

II. BACKGROUND AND EXAMPLES

In the limit of a large number of shots, the inverse error of the method-of-moments estimator of ϕ based on a total spin readout has the form

$$(\Delta\tilde{\phi})_{\vec{n}, \vec{m}}^{-2} = \frac{\left(\partial_\phi \langle \vec{m} \cdot \vec{J} \rangle_{|\psi_\phi(\vec{n})\rangle}\right)^2}{\text{Var}_{|\psi_\phi(\vec{n})\rangle} \vec{m} \cdot \vec{J}} \quad (6)$$

When the protocol has the form $|\psi_\phi\rangle = e^{-i\phi H} |\psi_0\rangle$ for some Hamiltonian H , it is often possible to simply take the $\phi \rightarrow 0$ limit of (6) by deriving expressions for the $\phi \rightarrow 0$ limits of the numerator and denominator and taking the quotient of these [13]. Unfortunately, this is not a valid approach for general protocols $|\psi_\phi\rangle$ due to the possibility of zeros appearing in the numerator and denominator. A full analysis of (6) in the $\phi \rightarrow 0$ limit involves the off-diagonal P function for quartic polynomials in J_+ and J_- . These amplitudes can be evaluated by the generating function method [16].

We now consider examples showing that at the extreme interaction times $t = 0, \pi/2$, combining a twist-untwist protocol (4) with a total spin readout gives a method-of-moments inverse error (6) that achieves the maximal QFI over all SU(2) rotation orbits of the one-axis twisted state $e^{-itJ_z^2} |\zeta = 1\rangle$ (at the same interaction times). First consider the classical sensing example of Yurke, et al. [17]. The state $|\sigma_\phi\rangle = e^{-i\phi J_z} |\zeta = 1\rangle$ is the $t = 0$ limit both for a one-axis twisting orbit of $|\zeta = 1\rangle$ and a twist-untwist protocol (4) (the sensing direction J_z was chosen

without loss of generality from the subspace spanned by J_z and J_y). One finds that, e.g.,

$$\frac{(\partial_\phi \langle J_x \rangle_{|\sigma_\phi\rangle})^2}{\text{Var}_{|\sigma_\phi\rangle} J_x} = \frac{\frac{N^2}{4} \sin^2 \phi}{\frac{N}{4} \sin^2 \phi} = N, \quad (7)$$

i.e., the error of the method-of-moments estimate obtained from J_x measurement achieves the standard quantum limit (SQL). This holds for all ϕ , even ϕ for which the numerator and denominator go to zero (although such points are experimentally unstable).

For the opposite extreme of $t = \pi/2$, consider the twist-untwist protocol state

$$\begin{aligned} |\psi_\phi\rangle &= e^{i\frac{\pi}{2}J_z^2} e^{-i\phi J_x} e^{-i\frac{\pi}{2}J_z^2} |\zeta = 1\rangle \\ &= \cos \frac{N\phi}{2} |\zeta = 1\rangle - \sin \frac{N\phi}{2} |\zeta = -1\rangle \end{aligned} \quad (8)$$

for even N (if N is odd, the rotation layer in (8) should be taken as $e^{-i\phi J_y}$, which gives the same form of final state as for N even). Then $\text{Var}_{|\psi_\phi\rangle} J_x = \frac{N^2}{4} \sin^2 N\phi$ and $(\partial_\phi \langle J_x \rangle_{|\psi_\phi\rangle})^2 = \frac{N^4 \sin^2 N\phi}{4}$ for all ϕ . It follows that $(\Delta\tilde{\phi})^2 = N^{-2}$ for all ϕ [18]. On the other hand, it is known that the state $e^{-i\frac{\pi}{2}J_z^2} |\zeta = 1\rangle$ has maximal QFI N^2 for the rotation $e^{-i\phi J_x}$ ($e^{-i\phi J_y}$) for N even (odd) [19, 20]. The fact that the twist-untwist protocol (8) allows to saturate Heisenberg limit using a total spin readout is remarkable because the state of the protocol is not even entangled for $\phi = \frac{k\pi}{N}$, $z \in \mathbb{Z}$. However, the signal $(\partial_\phi \langle J_x \rangle_{|\psi_\phi\rangle})^2$ diverges at these points, maintaining a constant value of $(\Delta\tilde{\phi})^2$. The main point is that on the interval $(0, \frac{\pi}{N})$, the state $|\psi_\phi\rangle$ follows a geodesic of the (collective) Bloch sphere, becoming distinguishable as fast as possible [21]. The present example also has the notable feature that the total spin readout J_x is optimal regardless of the parity of N due to the presence of the final untwist layer. By comparison, because the GHZ state $e^{-i\frac{\pi}{2}J_z^2} |+\rangle^{\otimes N}$ produced by one axis twisting is aligned on the x -axis (y -axis) for N even (odd), an optimal global readout as in (3) must be aligned with the respective rotation depending on the parity of N (viz., J_x rotation and $X^{\otimes N}$ readout (J_y rotation and $Y^{\otimes N}$ readout) is optimal for N even (odd)).

The examples in this section raise the question of whether a twist-untwist protocol and total spin readout can be constructed that saturate the maximal one-axis twisting QFI for interaction times t for $0 < t < \pi/2$. We analyze this full range of t in the next section. Finally, we note that our restriction to the one-axis twisting non-linear interaction is motivated by experiments in ultracold atomic gases in which one-axis twisted states are readily generated by manipulation of the two-body interaction. For other non-Gaussian states such as those in the twin-Fock manifold spanned by $|N/2, N/2\rangle$, $|N/2 - 1, N/2 + 1\rangle$, $|N/2 + 1, N/2 - 1\rangle$, it is known to be possible to achieve Heisenberg scaling $O(N^2)$ for the inverse error of method-of-moments estimator from a total

spin readout without implementing a twist-untwist protocol [17, 22]. Such states are not accessible from the one-axis twisting dynamics of $|\zeta = 1\rangle$ and we do not discuss these further.

III. QFI FOR GENERAL INTERACTION TIMES

Before we identify twist-untwist protocols and total spin readouts that saturate the maximal QFI of the one-axis twisted state $e^{-itJ_z^2} |\zeta = 1\rangle$ (over all rotation directions) for arbitrary interaction times t , it is important to understand how this maximal QFI scales with N for each t . Through the QCRI, the maximal QFI value sets a lower bound for the error one can hope to achieve using the state $e^{-itJ_z^2} |\zeta = 1\rangle$ for phase sensing. In fact, this maximal QFI is equal to the maximal QFI of (4) over all \vec{n} because the QFI does not depend on the untwisting layer. Therefore the QFI is the same for both (4) and $e^{-i\phi\vec{n}\cdot\vec{J}} e^{-itJ_z^2} |\zeta = 1\rangle$ with $\vec{n} = (\sin \xi \cos \theta, \sin \xi \sin \theta, \cos \xi)$. Specifically, the QFI is

$$\begin{aligned} &4\text{Var}_{e^{-itJ_z^2}|\zeta=1\rangle} (\sin \xi \cos \theta J_x + \sin \xi \sin \theta J_y + \cos \xi J_z) \\ &= \sin^2 \xi \left[\frac{N^2 + N}{2} + \frac{N(N-1)}{2} \cos 2\theta \cos^{N-2} 2t \right. \\ &\quad \left. - N^2 \cos^2 \theta \cos^{2(N-1)} t \right] \\ &\quad + N \cos^2 \xi \\ &\quad + \sin 2\xi [N(N-1) \sin \theta \cos^{N-2} t \sin t]. \end{aligned} \quad (9)$$

An analysis of the QFI for the special case $\vec{n} = (0, 1, 0)$ was given in [12]. The general features of the result of maximization over ξ and θ were discussed in [12, 23]. Note that the interaction time t , which can be alternatively written as χT where T is the real time and χ is the interaction strength, depends on N through the χ factor. The various scalings of t with N allow asymptotic analyses of the maximal QFI. We proceed to use (9) to derive the metrological phase diagram for rotation sensing with the states $e^{-itJ_z^2} |\zeta = 1\rangle$. Figure 1 shows the five regions of different maximal QFI scaling derived from the analysis of this section.

SQL scaling. Consider the interaction time $t = O(N^{-\alpha})$ with $\alpha > 1$, Using $\cos^N t \sim 1$ and $\sin t \sim \frac{1}{N^\alpha}$, one finds that the bracketed term in (9) scales as $O(N)$, the second term scales as $O(N)$, and the third term scales as $O(N^{2-\alpha})$. Therefore, the first and second terms dominate, but $O(N)$ is the maximum QFI that can be obtained. Specifically, the QFI is asymptotically $N(\sin^2 \xi \sin^2 \theta + \cos^2 \xi)$, from which one concludes that $\theta = \pm\pi/2$ and any ξ gives the asymptotic global optimum. This result also holds for ultrashort interaction times $o(N^{-\alpha})$, $\alpha > 1$. Logarithmic corrections to $t = O(N^{-\alpha})$ do not change this asymptotic value.

Sub-Heisenberg scaling. Now consider $t = O(N^{-\alpha})$

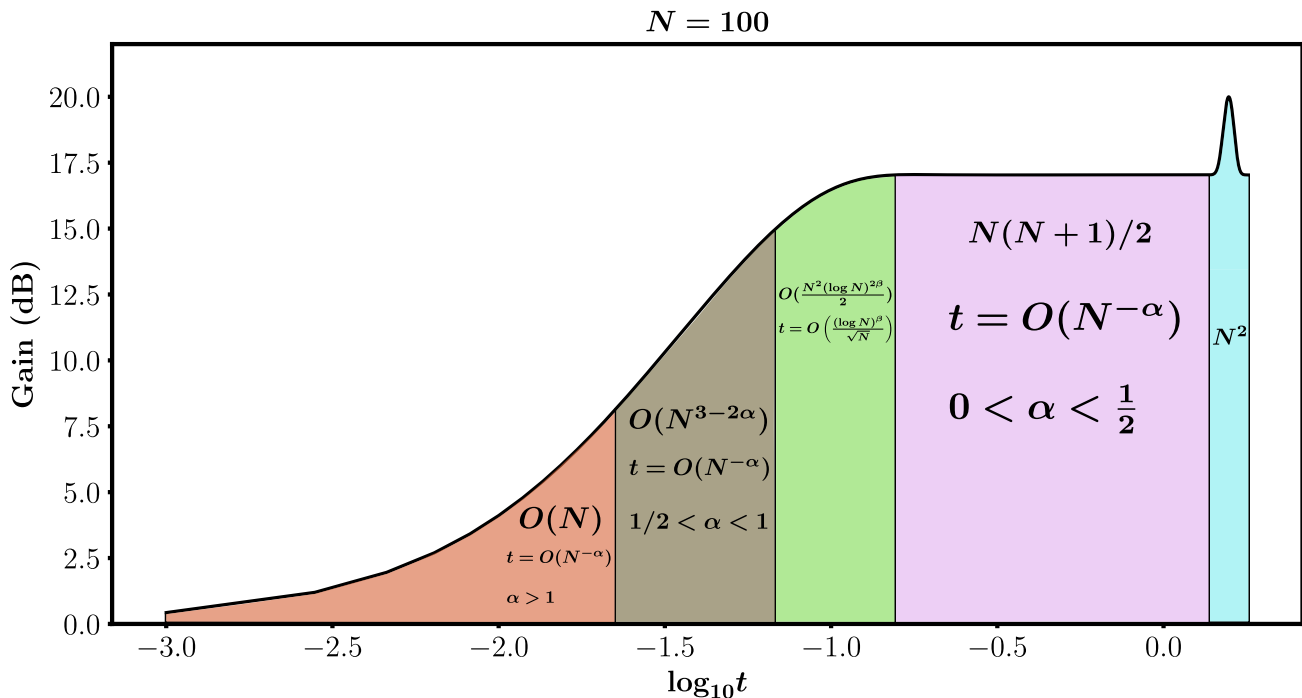


FIG. 1: Metrological phase diagram for the one-axis twisted state $e^{-itJ_z} |\zeta = 1\rangle$. The abscissa is the interaction time in units of Nt , $N = 100$. Note the log scale. There exists an interpolating interaction time scaling for adjacent phases. The QFI scaling as N^2 is associated with interaction time interval $[\frac{\pi}{2} - O(N^{-1/2}), \frac{\pi}{2} + O(N^{-1/2})]$. On a linear plot, the pink phase is nearly the whole time domain, as expected from Lemma 1.

for $1/2 < \alpha < 1$. Using $\cos^N t = 1 - \frac{Nt^2}{2} + O(t^4)$ and related second-order polynomial approximations to the trigonometric monomials in (9), one finds that the bracketed term in (9) scales as $O(N^{3-2\alpha})$, the second term scales as $O(N)$, and the third term scales as $O(N^{2-\alpha})$. Therefore, the term in brackets dominates for large N , and one finds the asymptotically optimal $\xi = \pi/2$, $\theta = \pi/2$. In particular, one obtains a maximal QFI of $O(N^{5/3})$ at $t = \frac{24^{1/6} 2^{2/3}}{2N^{2/3}}$, the time at which one-axis twisting generates maximal spin squeezing [1]. The dominance of the bracketed term persists for multiplicative logarithmic corrections to the $O(N^{-\alpha})$ scaling of t , and the QFI valued is correspondingly increased by a poly(log N) factor.

Heisenberg scaling. There are two interaction time domains that allow to achieve $O(N^2)$ QFI scaling which can be distinguished by their sensitivity to logarithmic corrections to the scaling of the interaction time. Consider first the case of an interaction time $t = O(N^{-\alpha})$, $0 < \alpha < 1/2$. It is clear that $\cos^N t \sim 0$, leading to an asymptotic QFI $\frac{N(N+1)}{2}$ for $\xi = \pi/2$ and arbitrary θ . These interaction times correspond to oversqueezing [1, 8, 14]. For large N , the atomic Husimi Q function for an oversqueezed one-axis twisting state has support on coherent states in a thin band surrounding the equator in the xy -plane, so it is not surprising that the maximal QFI is obtained independent of θ . Further, the independence of asymptotically optimal QFI on the azimuthal

angle implies that phase diffusion [24, 25] during the call to the sensing parameter θ does not affect optimal QFI in this phase.

Multiplicative logarithmic corrections to this interaction time scaling do not affect the asymptotics. Further, this range of interaction times, which interpolates between the oversqueezed and GHZ regimes, best reflects the expected metrological performance of one-axis twisting for interferometry. In particular,

$$\frac{2}{\pi} \int_0^{\frac{\pi}{2}} dt (9) \sim \sin^2 \xi \frac{N^2 + N}{2} + o(N^2) \quad (10)$$

which, due to convexity of the QFI, is an upper bound on the QFI of the uniform statistical mixture (over interaction times) of the states (4).

However, at smaller interaction times there is another scaling that leads to Heisenberg scaling of the QFI and encompasses the transition from sub-Heisenberg scaling to Heisenberg scaling. Consider the interaction time $t = O(\frac{(\log N)^\beta}{\sqrt{N}})$ with $\beta \in \mathbb{R}$. For $\beta = 0$, considering $t = \frac{c}{\sqrt{N}}$ results in an asymptotic QFI $N^2 \frac{1-e^{-2c^2}}{2}$ at the optimal angles $\xi = \theta = \pi/2$. This interaction time regime is where the properties of the twist-untwist protocol state with $\vec{n} = (0, 1, 0)$ have been most fully explored [2, 26]. For $\beta > 0$, this Heisenberg scaling is converted to the asymptotic Heisenberg scaling $N(N+1)/2$ discussed above. However, for $\beta < 0$, the optimal Heisenberg scaling is converted to optimal QFI of the form

$O(N^2(\log N)^{2\beta})$. The proof of this fact closely follows the discussion of sub-Heisenberg scaling above, simply noting that an interaction time $t = O(\frac{(\log N)^\beta}{\sqrt{N}})$, $\beta < 0$, still allows one to utilize the MacLaurin series for $\cos^N t$ at lowest nontrivial order. It follows that an interaction time scaling $t = O(\frac{(\log N)^\beta}{N^{1/2}})$ encompasses the transition to Heisenberg scaling.

Heisenberg limit. As mentioned below (9), the global maximum N^2 is obtained for $\xi = 0$. Combining this fact with the result from the Heisenberg scaling region, one concludes that the asymptotically optimal sensing direction for interaction times c/N^α with $\alpha \leq 1/2$ is in the linear span of J_x and J_y . The width of the GHZ region around $t = \frac{\pi}{2}$ is $O(1/\sqrt{N})$. This can be proved by showing that this neighborhood of $\frac{\pi}{2}$ interpolates between the Heisenberg limit N^2 and the $N^2/2$ QFI asymptotic calculated above for $t = O(N^{-\alpha})$, $0 < \alpha < 1/2$. Specifically, consider $t = \frac{\pi}{2} - \frac{c}{\sqrt{N}}$ for constant $c > 0$. From the fact that $\cos^N\left(\frac{\pi}{2} - \frac{c}{\sqrt{N}}\right) \rightarrow 0$, one finds that the third term (9) and the third term in brackets in the first line of (9) do not contribute, while the second term of (9) is $O(N)$. From the fact that $\cos^{N-2}\left(\pi - \frac{2c}{\sqrt{N}}\right) \sim \pm e^{-2c^2}$ (top (bottom) sign holds for N even (odd)), one finds that (9) is asymptotically

$$\sin^2 \xi \left[\frac{N^2}{2} \left(1 \pm \cos 2\theta e^{-2c^2}\right) + \frac{N}{2} \left(1 \mp \cos 2\theta e^{-2c^2}\right) \right]. \quad (11)$$

Taking $\xi = \pi/2$, $\theta = 0$ for N even and $\xi = \pi/2$, $\theta = \pi/2$ for N odd, this is the sought interpolation between N^2 (for small c) and $\frac{N^2+N}{2}$ (for large c). It is also worth noting that for constant interaction times $t = \frac{\pi}{m}$ ($m > 2$) defining discrete superpositions of equidistant coherent states [27], the asymptotically maximal QFI $N(N+2)/2$ is obtained with $\xi = \pi/2$ and arbitrary θ . This can be seen from the exponentially small contributions from $\cos t$ and $\cos 2t$ in (9) for constant $0 < t < \pi/2$.

The above analyses of the QFI scaling as a function of interaction time allows to draw the conclusion that the protocol (4) (or any protocol obtained from it by applying a ϕ -independent unitary) achieves its optimal metrological usefulness on the circle $\xi = \pi/2$, $\theta \in [-\pi, \pi]$, asymptotically in N . This useful corollary is not obvious from examination of a phase space distribution for (4), which is not aligned to a fixed direction on the sphere over all interaction times. Finally, we note that (10) suggests the hypothesis that the angles $\xi = \pi/2$, $\theta = 0$ are asymptotically almost everywhere optimal for all interaction times $t \in [0, \pi/2]$, and this QFI value is $\frac{N^2+N}{2}$. This hypothesis is true, and we provide a formal statement and proof.

Lemma 1. *For any $0 < \epsilon, \epsilon' < \pi/2$, there exists an N such that: 1. the maximum of (6) on an N -dependent interaction time interval $T_N \subset [0, \pi/2]$ is within ϵ' of $N(N+1)/2$, and 2. $|[0, \pi/2] \setminus T_N| < \epsilon$.*

Proof. Consider an interaction time of the form $\frac{\pi}{2} - \frac{c}{\sqrt{N}}$

with $0 < \beta < 1/2$. In this case, $\cos^N\left(\frac{\pi}{2} - \frac{c}{\sqrt{N}}\right) \rightarrow 0$ and $\cos^N\left(\pi - \frac{2c}{\sqrt{N}}\right) \rightarrow 0$; therefore, the first term in brackets in (6) dominates for large N . Depending on ϵ' , we then take N large enough that $\xi = \pi/2$ and arbitrary θ gives a value within ϵ' of $N(N+1)/2$. On the other hand, we derived above that for $\xi = \pi/2$, θ arbitrary, and interaction time $t = O(N^{-\alpha})$, $0 < \alpha < 1/2$, one can choose N sufficiently large that (9) is within ϵ' of $N(N+1)/2$. It follows that for $\epsilon' > 0$ and any $0 < \alpha, \beta < 1/2$ and any constants c, c' , one can choose a large enough N such that (9) is within ϵ' of $N(N+1)/2$ on the interval $T_N = [\frac{c}{\sqrt{N}}, \frac{\pi}{2} - \frac{c'}{\sqrt{N}}]$ for $\xi = \pi/2$ and arbitrary θ . Depending on ϵ , one then further increases N such that the difference between $[0, \pi/2]$ and this interval has measure ϵ . \square

The log scale for the interaction time in Figure 1 is used because it better illustrates the different phases. On a linear scale, the QFI is clearly seen to take the value $N(N-1)/2$ for almost the whole interaction time domain, as expected from Lemma 1.

IV. TWIST-UNTWIST PROTOCOLS

We now show that for $\phi \rightarrow 0$, the twist-untwist protocol with J_x rotation and a J_x measurement gives an error for the method-of-moments estimator of ϕ that is asymptotically equal to $N^2/2$ for interaction times $t = O(N^{-\alpha})$, $0 < \alpha < 1/2$. This conclusion holds regardless of the parity of N . Due to Lemma 1, this result implies that a twist-untwist protocol with total spin readout saturates the QCRI for one-axis twisting asymptotically for almost all interaction times (because the metrological phase diagram Fig.1 degenerates to the pink Heisenberg scaling phase).

To proceed, note that the denominator of (6) involves the derivative of the total spin signal, which can be written

$$\partial_\phi \langle \vec{m} \cdot \vec{J} \rangle_{|\psi_\phi(\vec{n})\rangle} = -2\text{Im} \langle \zeta = 1 | e^{itJ_z^2} \vec{n} \cdot \vec{J} e^{i\phi \vec{n} \cdot \vec{J}} e^{-itJ_z^2} \vec{m} \cdot \vec{J} | \psi_\phi \rangle \quad (12)$$

To analyse the $\phi \rightarrow 0$ behavior of this expression, one should calculate the MacLaurin expansion at least to $O(\phi)$ because the value of the expression may vanish at $\phi = 0$. We now show that for $t = O(N^{-\alpha})$, $0 < \alpha < 1$, $\max_{\vec{n}, \vec{m}} (\Delta \tilde{\phi})^2|_{\phi=0} \sim \frac{N(N+1)}{2}$ is obtained by taking $\vec{n} = \vec{m} = (1, 0, 0)$, i.e., J_x rotation and J_x readout. First note that for these values of \vec{n}, \vec{m} , (12) is zero at $\phi = 0$, so the $O(\phi^2)$ contribution to the denominator of (6) is the square of the $O(\phi)$ contribution to (12). One finds that to $O(\phi)$

$$\begin{aligned} \partial_\phi \langle J_x \rangle_{|\psi_\phi, \vec{n}\rangle} &= -N \phi \langle \zeta = 1 | e^{itJ_z^2} J_x^2 e^{-itJ_z^2} | \zeta = 1 \rangle \\ &+ 2\phi \langle \zeta = 1 | e^{itJ_z^2} J_x e^{-itJ_z^2} J_x e^{itJ_z^2} J_x e^{-itJ_z^2} | \zeta = 1 \rangle. \end{aligned} \quad (13)$$

The first line can be evaluated by a standard computation and the second line can be evaluated using Kitagawa-Ueda formulas and a table of third moments of the J_{\pm} operators in spin coherent states (see Appendix A). The result is in (A4). Taking $t = O(N^{\alpha})$, $0 < \alpha < 1/2$ gives

$$(\partial_{\phi} \langle J_x \rangle_{|\psi_{\phi}((1,0,0))\rangle})^2 \sim \frac{N^{6-4\alpha} \phi^2}{16}. \quad (14)$$

Unfortunately, the $O(\phi^2)$ contribution to the variance cannot be obtained from the same set of operator moments as (13), so a further calculation gives

$$\begin{aligned} \text{Var}_{|\psi_{\phi}((1,0,0))\rangle} J_x &= \frac{N\phi^2}{4} \langle e^{itJ_z^2} J_x^2 e^{-itJ_z^2} \rangle_{\zeta=1} \\ &+ \phi^2 \langle e^{itJ_z^2} J_x e^{-itJ_z^2} J_x^2 e^{itJ_z^2} J_x e^{-itJ_z^2} \rangle_{\zeta=1} \\ &- N\phi^2 \langle e^{itJ_z^2} J_x e^{-itJ_z^2} J_x e^{itJ_z^2} J_x e^{-itJ_z^2} \rangle_{\zeta=1} \\ &+ O(\phi^4). \end{aligned} \quad (15)$$

The first and last terms of (15) can be evaluated using expressions from (13), whereas the second term requires tabulation of fourth moments of J_{\pm} in spin coherent states (Appendix B). The final asymptotic result for the variance is

$$\text{Var}_{|\psi_{\phi}((1,0,0))\rangle} J_x = \frac{N^{4-4\alpha} \phi^2}{8}. \quad (16)$$

From the quotient of (13) and (16), one obtains the result

$$\frac{(\partial_{\phi} \langle J_x \rangle_{|\psi_{\phi}((1,0,0))\rangle})^2}{\text{Var}_{|\psi_{\phi}((1,0,0))\rangle} J_x} \Big|_{\phi=0} \sim \frac{N^2}{2}. \quad (17)$$

This equation proves that except for a set of interaction times of asymptotic measure zero, the $|\psi_{\phi}((1,0,0))\rangle$ twist-untwist protocol with J_x total spin readout saturates the quantum Cramér-Rao bound for one-axis twisting. One can also numerically verify for interaction times not in the pink phase of Fig. 1 that for large N , the optimal method-of-moments error for a twist-untwist protocol (6) saturates the one-axis twisting QCRI. Such optimal twist-untwist protocols are relevant for utilizing total spin readouts for sensing ϕ with a finite system size.

Because the one-axis twisting QFI is constant on a unitary path (defined only by the interaction time t and the rotation generator parameters ξ and θ defining \vec{n}), the one-axis twisting metrological phase diagram (1) and Lemma 1 are globally valid for all sensing angles ϕ . However, the results in this section only indicate that twist-untwist protocols near $\phi = 0$ exhibit the same maximal QFI as one-axis twisting. To extend the twist-untwist protocol (4) to a protocol that allows one to asymptotically saturate the one-axis twisting QCRI using the method-of-moments estimation from total spin readout (6) for any phase ϕ , it suffices to add a single controllable rotation after the call to the parameter ϕ :

$$|\tilde{\psi}_{\phi}(\vec{n})\rangle = e^{itJ_z^2} R e^{-i\phi \vec{n} \cdot \vec{J}} e^{-itJ_z^2} |\zeta = 1\rangle \quad (18)$$

where R is a parametrized $SU(2)$ operation which can be optimized over, analogously to the realigning pulses in a trapped Bragg interferometry sequence [28]. Since R is independent of ϕ , $|\tilde{\psi}_{\phi}(\vec{n})\rangle$ has the same QFI as (4) or the one-axis twisted state $e^{-i\phi \vec{n} \cdot \vec{J}} e^{-itJ_z^2} |\zeta = 1\rangle$. Mathematically, it is clear that taking $R = e^{i\phi' \vec{n} \cdot \vec{J}}$ is the same as evaluating (6) at $\phi' - \phi$. Scanning ϕ' then allows to obtain the $\phi = 0$ method-of-moments error, but for any ϕ . In a Mach-Zehnder interferometry sequence, one takes $\vec{n} \cdot \vec{J} = J_x$ or J_y , and the phase ϕ is imprinted as a phase shift of modes via $e^{-i\phi J_y(J_x)} = e^{-i\frac{\pi}{2} J_x(-J_y)} e^{i\phi J_z} e^{i\frac{\pi}{2} J_x(-J_y)}$, so for a general phase ϕ , a protocol that asymptotically saturates the one-axis twisting QCRI is

$$e^{itJ_z^2} e^{i\phi' J_y(J_x)} e^{-i\frac{\pi}{2} J_x(-J_y)} e^{-i\phi \vec{n} \cdot \vec{J}} e^{i\frac{\pi}{2} J_x(-J_y)} e^{-itJ_z^2} |\zeta = 1\rangle. \quad (19)$$

with J_x or J_y chosen according to the asymptotically optimal ξ, θ pair derived in Section III for any given interaction time t .

One undesirable aspect of the optimal twist-untwist protocol in both Heisenberg scaling phases, in the sub-Heisenberg scaling phase, and also in the small Heisenberg limit phase near interaction time $\pi/2$, is the fact that the optimal twist-untwist protocol utilizes a signal $\langle J_x \rangle_{|\psi_{\phi}\rangle}$ which has zero derivative with respect to ϕ at $\phi = 0$. In practice, this behavior leads to unstable behavior of the method of moments estimator of ϕ in a neighborhood of zero. A potential route to circumvent this aspect of the optimal twist-untwist protocol is to utilize (18). For example, considering $t = 1/\sqrt{N}$, the optimal ϕ rotation direction in the twist-untwist protocol is J_y , and the optimal readout is J_x , but according to (18), one lets R be a tunable non-identity rotation. Because the signal would have non-zero derivative, the experiment can tune R to be as close to the identity as possible while still getting Heisenberg scaling for the method of moments estimate of ϕ .

V. FINITE-RANGE ONE-AXIS TWISTING

Consider $N + 2$ spin-1/2 particles interacting on a 1-D lattice with periodic boundary conditions according to the interaction Hamiltonian

$$H_K = \frac{1}{4} \sum_{j=1}^{N+2} \sum_{\substack{i=j-K \\ i \neq j}}^{j+K} Z_i Z_j \quad (20)$$

where Z_i is the Pauli Z matrix on site i . Such an interaction corresponds to a uniform coupling of the spins over a range $2K$. We take $N \equiv 0 \pmod{2}$ and note that $H_{N/2} + \frac{1}{4} \sum_{j=1}^N Z_j Z_{j+1+\frac{N}{2} \pmod{N}} = 2J_z^2$ with J_z in a $j = \frac{N+2}{2}$ representation of $\mathfrak{su}(2)$. Surprisingly, removing the antipodal interaction and considering just the long range one-axis twisting interaction $H_{N/2}$ produces a metrological phase diagram that qualitatively differs from Fig. 1.

TABLE I: Metrological phases for finite-range one-axis twisting. The second, third, and fourth columns show the scaling of the interaction time that defines the metrological phase.

Interaction range	SQL	SQL-Heisenberg interpolation	Heisenberg
$1 \leq K \leq \frac{N}{4}$	$\Omega\left(\frac{(\log K)^\beta}{K^\alpha}\right); \alpha > 1/2, \beta \geq 0$	$\Omega\left(\frac{(\log K)^\beta}{K^\alpha}\right); 0 < \alpha \leq 1/2, \beta > 0$ $O(1), \pi/2$ included	$\Omega(K^{-1/2}), K = \lambda N$
$K = \frac{N}{2}$	$\Omega\left(\frac{(\log N)^\beta}{N^\alpha}\right); \alpha > 1/2, \beta \geq 0$ $\frac{\pi}{2} - O(N^{-1/2})$ (doubled SQL)	$\Omega\left(\frac{(\log N)^\beta}{N^\alpha}\right); 0 < \alpha \leq 1/2, \beta > 0$ $O(1), \pi/2$ not included	$\Omega(N^{-1/2})$

We start by deriving a metrological phase diagram for finite-range one-axis twisting generated by H_K in the case $1 \leq K \leq \frac{N}{4}$. The QFI on the path $e^{-i\phi\vec{n}\cdot\vec{J}}$ is in (C2). From (C2) one can see that the QFI for finite range one-axis twisting is determined by rational trigonometric functions, with growth determined by the function $\cos^K mt$, $m = 1, 2$. We therefore consider the interaction time to scale in various ways with respect to K , and take the large K limit, always noting that N must be taken greater than or equal to $4K$. One should note that if the range K is fixed, there is no hope for $O((N+2)^2)$ scaling of the QFI. From (C2), one sees that the $O((N+2)^2)$ term simplifies to zero, regardless of the readout $\vec{n}\cdot\vec{J}$. Therefore, any $O(N^2)$ scaling would come from taking K to scale linearly with N (with slope $\leq 1/4$).

SQL scaling. There is a single metrological phase exhibiting strict SQL scaling when $1 \leq K \leq \frac{N}{4}$. Consider $t(K) = \frac{c(\log K)^\beta}{K^\alpha}$ with $\alpha > 1/2, \beta \geq 0$. We have $\cos^K t(K) \sim 1$, and applying L'Hopital's rule to (C2), one obtains that the QFI is

$$(N+2)(\cos^2 \xi - \sin^2 \xi \cos 2\theta) \quad (21)$$

for large K , which implies that taking $\xi = 0$ (the path generated by J_z) or $\xi = \frac{\pi}{2}, \theta = \pi$ (the path generated by J_y) achieves SQL. This is consistent with the two paths that give QFI equal to N for the $t = 0$ non-spin-squeezed state $|+\rangle^{\otimes N}$.

Heisenberg-SQL interpolation. We have already established that when $1 \leq K \leq \frac{N}{4}$, $O(N^2)$ scaling of the QFI cannot occur for fixed K . However, there is the possibility that the QFI scales as $O(NK^{2\alpha})$ for large K , which induces Heisenberg scaling for $\alpha = 1/2$ and $K = \lambda N$ (with $0 < \lambda < \frac{1}{4}$ because we are considering $1 \leq K \leq \frac{N}{4}$). To investigate this possibility, consider any scaling $t(K)$ such that $\cos^K t(K) \rightarrow 0$, e.g., $t(K) = \frac{c(\log K)^\beta}{K^\alpha}$, $0 < \alpha \leq 1/2, \beta > 0$, or constant scaling $t = c \in (0, \frac{\pi}{2}]$. In this case, the QFI is

$$\frac{N+2}{\sin^2 t(K)} \sin^2 \xi + (N+2) \cos^2 \xi, \quad (22)$$

which for large K is maximized by $\xi = \frac{\pi}{2}$ regardless of θ , with corresponding value $\frac{N+2}{\sin^2 t(K)}$. The scaling in (22) is shown in Fig. 2. For large K , this functional form fills out the entire metrological phase diagram. Using form of

$t(K)$ above, one notes that the QFI on a rotation path defined by \vec{n} in the xy -plane is asymptotically $\frac{(N+2)K^{2\alpha}}{c^2(\log K)^{2\beta}}$ for large K , which corresponds to Heisenberg scaling if an aspect ratio $0 < \lambda \leq \frac{1}{4}$ is defined where $K = \lambda N$. By contrast, taking a constant t (which is interpolated by the form of $t(K)$) gives SQL scaling. Therefore, these interaction time scalings interpolate between Heisenberg scaling and SQL scaling of the QFI.

Heisenberg scaling. Because logarithmic corrections to $t = \Omega(K^{-1/2})$ scaling are already covered in the analyses above, it only remains to analyze $t = \frac{c}{\sqrt{K}}$ with $c > 0$, i.e., $\beta = 0$ and $\alpha = 1/2$ in $t(K)$. To do this, we neglect the terms that do not scale with both N and K (the $O(N^2)$ term vanishes identically, so this actually amounts to neglecting $O(N)$ terms). The QFI is

$$\frac{(N+2)K \sin^2 \xi}{4} \left(\frac{1 - e^{-2c^2}}{c^2} - 2e^{-2c^2} + \cos 2\theta \left(\frac{e^{-2c^2} - e^{-4c^2}}{c^2} - 2e^{-2c^2} \right) \right) \quad (23)$$

maximized for $\xi = \theta = \pi/2$ regardless of c . This $O((N+2)K)$ scaling of the QFI is the best possible for short, finite-range one axis twisting, and corresponds to Heisenberg scaling when an aspect ratio λ is chosen. Calculations of the QFI (optimized over all directions) for two-dimensional, finite-range one-axis twisting with a $1/r_{ij}^6$ potential relevant to lattice Rydberg atoms further confirm that, unlike the case for one-axis twisting, a QFI greater than SQL does not persist beyond a short regime of interaction times [29]. The same work also shows an asymptotic scaling NK^γ of the QFI, where $\gamma \approx 1.94$ and where K represents the range of the interaction as a multiple of the lattice spacing. Along with (23), which show an $O(NK)$ scaling in the one-dimensional setting, this suggests a dimensionality dependence of the maximal QFI $\propto NK^{O(d)}$ for short finite-range one-axis twisting in dimension d .

Finally, we derive a metrological phase diagram for finite-range one-axis twisting generated by H_K in the case $\frac{N}{4} < K \leq \frac{N}{2}$. The QFI on the path $e^{-i\phi\vec{n}\cdot\vec{J}}$ is in (C3). Unlike the case for $\frac{N}{4} < K \leq \frac{N}{2}$, the exponents in the rational trigonometric functions are not just multiples of K , so it is unclear how to choose the scalings of the interaction times. A totally general analysis would

define an aspect ratio $K = \lambda N$ with $\frac{1}{4} < \lambda \leq \frac{1}{2}$ and for each λ consider interaction time scaling with N . However, the most interesting question concerning quantum metrology with long finite-range one-axis twisting interaction is whether the metrological phase diagram interpolates to that of the J_z^2 interaction (i.e., the bosonic case) for $\lambda = 1/2$. Therefore, we take $\lambda = 1/2$ and analyze the interaction time scaling with N .

SQL scaling. There are two disjoint metrological phases that correspond to SQL scaling. First, consider interaction time scaling $t(N) = \frac{c(\log N)^\beta}{N^\alpha}$, $\alpha > 1/2$, $\beta \geq 0$. We have $\cos^N t(N) \sim 1$ and applying L'Hopital's rule to (C3), one obtains that the QFI is

$$(N+2) \left(\frac{5 \sin^2 \xi}{2} + \frac{3 \sin^2 \xi \cos 2\theta}{2} + \cos^2 \xi - 4 \sin^2 \xi \cos^2 \theta \right). \quad (24)$$

This is maximized for $\xi = 0$ (J_z generator), or $\xi = \pi/2$, $\theta = \pi/2$ (J_y generator), with maximal value $(N+2)$ in both cases. Second, consider $t = \frac{\pi}{2}$ which gives QFI

$$(N+2) \left(\frac{3 \sin^2 \xi}{2} + \frac{\sin^2 \xi \cos 2\theta}{2} + \cos^2 \xi \right). \quad (25)$$

This obtains maximum $2(N+2)$ for $\xi = \frac{\pi}{2}$, $\theta = 0$. This "doubled SQL" scaling persists for interaction time scaling $t(N) = \frac{\pi}{2} - \frac{c}{\sqrt{N}}$, $c > 0$. Note that if N is odd, the optimal θ is $\pi/2$ instead of 0.

Heisenberg-SQL interpolation. Consider interaction time $t(N)$ scaling with N in such a way that $\cos^N t(N) \rightarrow 0$. For example, $t(N) = \frac{c(\log N)^\beta}{N^\alpha}$ with $0 < \alpha \leq \frac{1}{2}$ and $\beta > 0$, or constant $t = c \in (0, \frac{\pi}{2}]$. In this case, (C3) is asymptotically independent of θ and the QFI is then given by

$$\frac{\sin^2 \xi}{8} \left(\cos^2 t(N)(N^2 - 4) + 2(N+2) \left(\frac{1 - \cos^4 t(N)}{\sin^2 t(N)} \right) + N + 2 \right) + \frac{N+2}{4} \cos^2 \xi \quad (26)$$

which obtains its maximum value

$$\frac{N^2 - 4}{2} \cos^2 t(N) + \frac{N+2}{2} (3 + 2 \cos^2 t(N)) \quad (27)$$

at $\xi = \pi/2$. This scaling form interpolates between Heisenberg scaling and the doubled SQL scaling. For $N+2 = 100$, Fig. 2 compares this scaling form to the maximal QFI on the path generated by $\vec{n} \cdot \vec{J}$ over all \vec{n} . One can see the two SQL scaling phases on the left and right that this functional form of the QFI does not describe. Note that the Heisenberg limit regime in a neighborhood of $\frac{\pi}{2}$ that occurs in the case of the bosonic one-axis twisting generator J_z^2 (i.e., all-to-all pairwise interactions of equal strength) does not exist for long,

finite-range one-axis twisting even in the extreme case of $K = N/2$. In other words, full connectivity of interactions is necessary for achieving the Heisenberg limit.

Heisenberg scaling. Because logarithmic corrections to $t = \Omega(N^{-1/2})$ scaling are covered by the previous regimes, it only remains to consider $t(N) = \frac{c}{\sqrt{N}}$. Plugging this scaling into (C3) gives QFI

$$\frac{N^2 \sin^2 \xi}{2} (1 + e^{-2c^2} \cos 2\theta - 2e^{-c^2} \cos^2 \theta) + o(N^2) \quad (28)$$

which has a unique maximum $\frac{N^2(1-e^{-2c^2})}{2}$ at $\xi = \theta = \pi/2$.

For both short and long finite-range one-axis twisting, the only range of interaction times that are relevant in the $K \rightarrow \infty$ with $K = \lambda N$ are captured by the Heisenberg-SQL scaling interpolations in (22), (26), respectively. Therefore, unlike bosonic one-axis twisting which has only one asymptotic metrological phase described by Lemma 1, finite-range one-axis twisting asymptotically has two metrological phases which are connected by the scaling forms in (22), (26) for the short range and long range cases, respectively.

A. Finite-range twist-untwist protocols

In Ref.[26], the short finite-range ($K \leq N/4$) twist-untwist protocol with J_y rotation and J_y readout was determined to asymptotically attain, at its optimal interaction time, 92% of the one-axis twisting quantum Fisher information in the J_y direction at that same interaction time. That interaction time is in the Heisenberg scaling metrological phase defined by the interaction time scaling $t = \frac{c}{K^{1/2}}$. However, that work did not determine whether the best possible twist-untwist protocol (defined by optimal \vec{n} and \vec{m}) can saturate the short finite-range one-axis twisting QFI on its optimal rotation path, which, as we showed in the previous subsection, is indeed generated by J_y . Ideally, to answer this question, one would use the analytical approach of Section IV to identify the optimal \vec{n}, \vec{m} that allow a twist-untwist protocol to get as close as possible to the maximal value of (23) for this $t = O(K^{-1/2})$ metrological phase.

However, in the analysis of Section IV, it was efficient to compute the $\phi \rightarrow 0$ limit of the empirical error $(\Delta\tilde{\phi})^2$ for the twist-untwist protocol defined by J_x rotation and J_x readout because when the one-axis twisting is generated by J_z^2 , one can compute the small- ϕ expansions of the numerator and denominator of $(\Delta\tilde{\phi})^2$ by using the third and fourth moments of spin operators in SU(2) coherent states, which are easily derived. In contrast, the states that arise in the analogous calculation with a finite-range one-axis twisting generator H_K are not restricted to the manifold of SU(2) coherent states, so calculating the third and fourth moments of the set $\{J_z, J_+, J_-\}$ for finite-range one-axis twist-untwist dynamics is considerably more complicated. We therefore

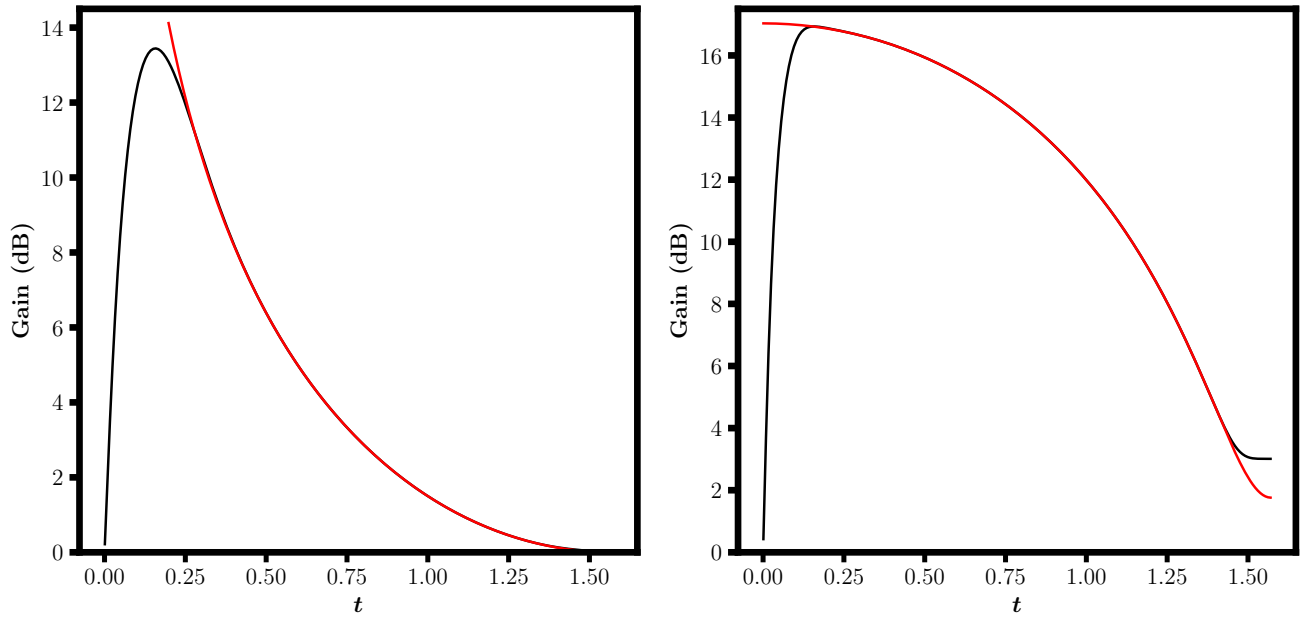


FIG. 2: (Left) Red: (22) for $t \in (0.2, \pi/2)$ for $N + 2 = 100$, Black: $\frac{4}{N+2} \max_{\vec{n}} \text{Var} \vec{n} \cdot \vec{J}$ (in decibels) in the state $e^{-itH_K} |+\rangle^{\otimes N+2}$ on $t \in (0, \pi/2)$, with $K = (N + 2)/4$ and $N + 2 = 100$ (Right) Red: (27) for $t \in (0, \pi/2)$ for $N + 2 = 100$, Black: $\frac{4}{N+2} \max_{\vec{n}} \text{Var} \vec{n} \cdot \vec{J}$ (in decibels) in the state $e^{-itH_K} |+\rangle^{\otimes N+2}$ on the same interaction time interval, with $K = (N + 2)/2$ and $N + 2 = 100$.

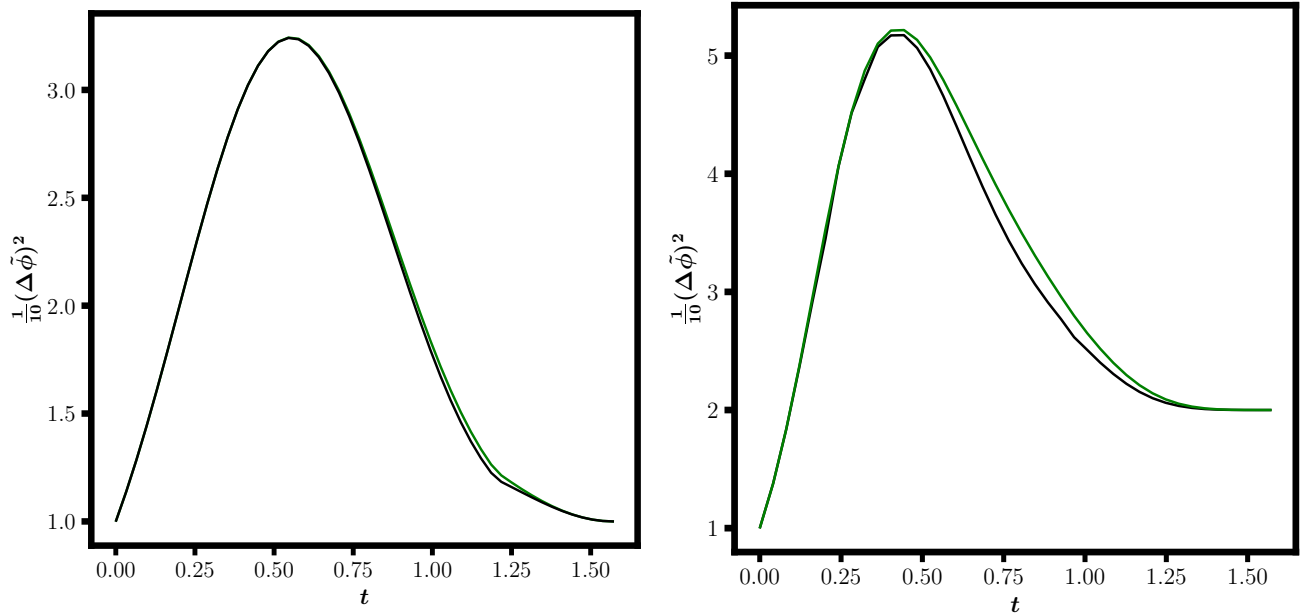


FIG. 3: Comparison of maximal QFI for finite range, one-axis twisting (green) and maximal reciprocal of the method-of-moments error for a twist-untwist protocol with finite-range, one-axis twisting (black). Both values are multiplied by N^{-1} so that the SQL corresponds to value 1. $N + 2 = 10$, $K = \frac{N}{4} = 2$ (left); $N + 2 = 10$, $K = \frac{N}{2} = 4$ (right). $(\Delta \tilde{\phi}^2)_{\vec{n}, \vec{m}}$ is optimized over \vec{n} and \vec{m} at $\phi = 10^{-3}$ so that the computer program returns a finite result.

provide numerical evidence in Fig. 3 for $N + 2 = 10$, that for $K = \frac{N}{4}$ in the short range case and $K = \frac{N}{2}$ in the long range case that there is a finite-range twist-

untwist protocol that saturates (differs by less than N^{-1}) the QFI in the Heisenberg scaling phase. In the case of short finite-range twist-untwist, the optimal proto-

col the optimal protocol at the optimal interaction time on the time grid is given by rotation generator $\vec{n} \cdot \vec{J}$ with $\vec{n} = (0.86559, 0.00020, 0.50076)$ and measurement of $\vec{m} \cdot \vec{J}$ with $\vec{m} = (-0.99999, 0.00033, -0.00009)$, whereas in the case of long finite-range twist-untwist, the optimal protocol at the optimal interaction time on the time grid is given by rotation generator $\vec{n} \cdot \vec{J}$ with $\vec{n} = (0.00010, 0.92735, 0.37419)$ and measurement of $\vec{m} \cdot \vec{J}$ with $\vec{m} = (-0.99999, 0.00044, -0.00009)$. In both cases, the vectors \vec{n} and \vec{m} were optimized over the hemisphere $\theta \in (0, \pi)$, $\varphi \in (0, \pi)$.

ACKNOWLEDGMENTS

The authors were supported by the Laboratory Directed Research and Development (LDRD) program of

Los Alamos National Laboratory (LANL) under project number 20210116DR. Michael J. Martin was also supported by supported by the U.S. Department of Energy, Office of Science, National Quantum Information Science Research Centers, Quantum Science Center. Los Alamos National Laboratory is managed by Triad National Security, LLC, for the National Nuclear Security Administration of the U.S. Department of Energy under Contract No. 89233218CNA000001.

-
- [1] Masahiro Kitagawa and Masahito Ueda, “Squeezed spin states,” *Phys. Rev. A* **47**, 5138–5143 (1993).
- [2] Emily Davis, Gregory Bentsen, and Monika Schleier-Smith, “Approaching the Heisenberg Limit without Single-Particle Detection,” *Phys. Rev. Lett.* **116**, 053601 (2016).
- [3] S. C. Burd, R. Srinivas, J. J. Bollinger, A. C. Wilson, D. J. Wineland, D. Leibfried, D. H. Slichter, and D. T. C. Allcock, “Quantum amplification of mechanical oscillator motion,” *Science* **364**, 1163 (2019).
- [4] S. Colombo, E. Pedrozo-Penafiel, A. F. Adiyatullin, Z. Li, E. Mendez, C. Chi Shu, and V. Vuletic, “Time-Reversal-Based Quantum Metrology with Many-Body Entangled States,” *Nat. Phys.* -, - (2022).
- [5] D. Linnemann, H. Strobel, W. Muessel, J. Schulz, R. J. Lewis-Swan, K. V. Kheruntsyan, and M. K. Oberthaler, “Quantum-enhanced sensing based on time reversal of nonlinear dynamics,” *Phys. Rev. Lett.* **117**, 013001 (2016).
- [6] Marius Schulte, Victor J. Martínez-Lahuerta, Maja S. Scharnagl, and Klemens Hammerer, “Ramsey interferometry with generalized one-axis twisting echoes,” *Quantum* **4**, 268 (2020).
- [7] Vittorio Giovannetti, Seth Lloyd, and Lorenzo Maccone, “Quantum metrology,” *Phys. Rev. Lett.* **96**, 010401 (2006).
- [8] Luca Pezzè, Augusto Smerzi, Markus K. Oberthaler, Roman Schmied, and Philipp Treutlein, “Quantum metrology with nonclassical states of atomic ensembles,” *Rev. Mod. Phys.* **90**, 035005 (2018).
- [9] H. Lee, P. Kok, and J. P. Dowling, “A quantum rosetta stone for interferometry,” *J. Mod. Opt.* **49**, 14 (2002).
- [10] Samuel P. Nolan, Stuart S. Szigeti, and Simon A. Haine, “Optimal and robust quantum metrology using interaction-based readouts,” *Phys. Rev. Lett.* **119**, 193601 (2017).
- [11] L. I. R. Gil, R. Mukherjee, E. M. Bridge, M. P. A. Jones, and T. Pohl, “Spin Squeezing in a Rydberg Lattice Clock,” *Phys. Rev. Lett.* **112**, 103601 (2014).
- [12] Luca Pezzè and Augusto Smerzi, “Entanglement, Nonlinear Dynamics, and the Heisenberg Limit,” *Phys. Rev. Lett.* **102**, 100401 (2009).
- [13] Manuel Gessner, Augusto Smerzi, and Luca Pezzè, “Metrological nonlinear squeezing parameter,” *Phys. Rev. Lett.* **122**, 090503 (2019).
- [14] Y. Baamara, A. Sinatra, and M. Gessner, “Squeezing of nonlinear spin observables by one axis twisting in the presence of decoherence: An analytical study,” *Comptes Rendus. Physique* **23**, 1 (2022).
- [15] Youcef Baamara, Alice Sinatra, and Manuel Gessner, “Scaling laws for the sensitivity enhancement of non-gaussian spin states,” *Phys. Rev. Lett.* **127**, 160501 (2021).
- [16] F. T. Arecchi, Eric Courtens, Robert Gilmore, and Harry Thomas, “Atomic coherent states in quantum optics,” *Phys. Rev. A* **6**, 2211–2237 (1972).
- [17] Bernard Yurke, Samuel L. McCall, and John R. Klauder, “SU(2) and SU(1,1) interferometers,” *Phys. Rev. A* **33**, 4033–4054 (1986).
- [18] G. S. Agarwal, *Quantum Optics* (Cambridge, UK, 2013).
- [19] B. Yurke and D. Stoler, “Generating quantum mechanical superpositions of macroscopically distinguishable states via amplitude dispersion,” *Phys. Rev. Lett.* **57**, 13–16 (1986).
- [20] Barry C. Sanders, “Quantum dynamics of the nonlinear rotator and the effects of continual spin measurement,” *Phys. Rev. A* **40**, 2417–2427 (1989).
- [21] T.J. Volkoff and K.B. Whaley, “Distinguishability times and asymmetry monotone-based quantum speed limits in the Bloch ball,” *Quantum* **2**, 96 (2018).
- [22] Taesoo Kim, Olivier Pfister, Murray J. Holland, Jaewoo Noh, and John L. Hall, “Influence of decorrelation on heisenberg-limited interferometry with quantum correlated photons,” *Phys. Rev. A* **57**, 4004–4013 (1998).
- [23] K. Gietka, P. Szańkowski, T. Wasak, and J. Chwedeńczuk, “Quantum-enhanced interferometry and the structure of twisted states,” *Phys. Rev. A* **92**, 043622 (2015).

- [24] Juha Javanainen and Martin Wilkens, “Phase and phase diffusion of a split bose-einstein condensate,” *Phys. Rev. Lett.* **78**, 4675–4678 (1997).
- [25] Ebubekukwu O. Ilo-Okeke and Alex A. Zozulya, “Atomic population distribution in the output ports of cold-atom interferometers with optical splitting and recombination,” *Phys. Rev. A* **82**, 053603 (2010).
- [26] T. J. Volkoff and Michael J. Martin, “Asymptotic optimality of twist-untwist protocols for heisenberg scaling in atom-based sensing,” *Phys. Rev. Research* **4**, 013236 (2022).
- [27] “production of schrödinger macroscopic quantum-superposition states in a kerr medium,” .
- [28] Robin Corgier, Luca Pezzè, and Augusto Smerzi, “Non-linear Bragg interferometer with a trapped Bose-Einstein condensate,” *Phys. Rev. A* **103**, L061301 (2021).
- [29] Tommaso Macrì, Augusto Smerzi, and Luca Pezzè, “Loschmidt echo for quantum metrology,” *Phys. Rev. A* **94**, 010102 (2016).
- [30] X. Wang and K. Molmer, “Pairwise entanglement in symmetric multi-qubit systems,” *Eur. Phys. J. D* **18**, 385 (2002).
- [31] Xiaoguang Wang and Barry C. Sanders, “Spin squeezing and pairwise entanglement for symmetric multiqubit states,” *Phys. Rev. A* **68**, 012101 (2003).

Appendix A: Calculation of (13)

The first line of (13) is a standard computation (see second moments of spin operators in SU(2) coherent states [30, 31]) and yields

$$-N\phi \text{Re}\langle \zeta = 1 | e^{itJ_z^2} J_x^2 e^{-itJ_z^2} | \zeta = 1 \rangle = -N\phi \left(\frac{N^2 + N}{8} + \frac{N(N-1)}{8} \cos^{N-2} 2t \right). \quad (\text{A1})$$

The second line of (13) is given by

$$\begin{aligned} & 2\phi \text{Re}\langle \zeta = 1 | e^{itJ_z^2} J_x e^{-itJ_z^2} J_x e^{itJ_z^2} J_x e^{-itJ_z^2} | \zeta = 1 \rangle = \\ & \frac{\phi}{4} \text{Re}\langle \zeta = 1 | \left(e^{2it(J_z - \frac{1}{2})} J_+ + e^{-2it(J_z + \frac{1}{2})} J_- \right) (J_+ + J_-) \left(J_+ e^{2it(J_z + \frac{1}{2})} + J_- e^{-2it(J_z - \frac{1}{2})} \right) | \zeta = 1 \rangle \\ & = \frac{\phi}{4} \text{Re} \left[\langle \zeta = e^{2it} | J_+^3 + J_+ J_- J_+ | \zeta = e^{-2it} \rangle + c.c. \right. \\ & \quad \left. + \langle \zeta = e^{2it} | J_+^2 J_- | \zeta = e^{2it} \rangle + c.c. \right. \\ & \quad \left. + \langle \zeta = e^{-2it} | J_- J_+^2 | \zeta = e^{-2it} \rangle + c.c. \right] \\ & = \frac{\phi}{4} \left[\frac{N(N-1)(N-2)}{2} \cos^{N-3} 2t + N^2 \cos^{N-1} 2t + 2N(N-1) \cos 2t + \frac{N(N-1)(N-2)}{2} \cos 2t \right]. \end{aligned} \quad (\text{A2})$$

So the full result for (13) is

$$\partial_\phi \langle J_x \rangle_{|\psi_\phi((1,0,0))\rangle} = -\frac{N\phi}{8} (N^2 + N + N(N-1) \cos^{N-2} 2t) + (\text{A3}) + O(\phi^3). \quad (\text{A4})$$

Taking $t = \frac{c}{N^\alpha}$, $0 < \alpha < 1/2$ gives

$$\begin{aligned} (\partial_\phi \langle J_x \rangle_{|\psi_\phi((1,0,0))\rangle})^2 & \sim \left(\left(\frac{N^3}{8} + \frac{N^2}{8} \right) (1 - \cos 2t) - \frac{N}{4} \cos 2t \right)^2 \\ & \sim \left(N^3 \sin^2 \frac{c}{N^\alpha} + N^2 \sin^2 \frac{c}{N^\alpha} + N \cos \frac{2c}{N^\alpha} \right)^2 \frac{\phi^2}{16} \end{aligned} \quad (\text{A5})$$

Appendix B: Calculation of J_{\pm} moments for (16)

Using the results of Appendix A, (15) is simplified to

$$\begin{aligned} \phi^{-2} \text{Var}_{|\psi_{\phi}((1,0,0))\rangle} J_x &= \frac{N^4}{32} + \frac{N^3}{32} + \left(\frac{N^4}{16} + \frac{N^3}{16} - \frac{N^2}{8} \right) \cos 2t \\ &\quad + \langle e^{itJ_z^2} J_x e^{-itJ_z^2} J_x^2 e^{itJ_z^2} J_x e^{-itJ_z^2} \rangle_{|\zeta=1\rangle} \\ &\quad + O(\phi^2). \end{aligned} \tag{B1}$$

Since for $t = \frac{c}{N^\alpha}$, $0 < \alpha < 1/2$, it follows that $\cos^N t \rightarrow 0$, one finds that the second line of (B1) has the asymptotic form

$$\begin{aligned} \langle e^{itJ_z^2} J_x e^{-itJ_z^2} J_x^2 e^{itJ_z^2} J_x e^{-itJ_z^2} \rangle_{|\zeta=1\rangle} &\sim \frac{1}{16} \langle J_+^3 J_- + J_+ J_- J_+ J_- + J_+^2 J_-^2 + J_+ J_-^3 \rangle_{|\zeta=e^{2it}\rangle} \\ &\quad + \frac{1}{16} \langle J_- J_+^3 + J_-^2 J_+^2 + J_- J_+ J_- J_+ + J_-^3 J_+ \rangle_{|\zeta=e^{-2it}\rangle} \\ &\sim \frac{N^4}{64} (1 + \cos 4t). \end{aligned} \tag{B2}$$

Substituting this result into (B1) and taking $t = \frac{c}{N^\alpha}$, $0 < \alpha < 1/2$ gives

$$\text{Var}_{|\psi_{\phi}((1,0,0))\rangle} J_x \sim \frac{N^4 \phi^2}{8} \sin^4 \frac{c}{N^\alpha} \tag{B3}$$

which gives (16) for large N .

Appendix C: QFI for finite-range one-axis twisting

$N + 2$ atoms on a ring, N even. We use

$$\begin{aligned} \text{Var}_{e^{-itH_K|+}\rangle^{\otimes N}} (\sin \xi \cos \theta J_x + \sin \xi \sin \theta J_y + \cos \xi J_z) &= \frac{\sin^2 \xi}{2} (\text{Re}(e^{2i\theta} \langle J_-^2 \rangle) + \langle J_- J_+ \rangle) \\ &\quad + \frac{\sin 2\xi}{2} (\text{Re}(e^{i\theta} \langle J_z J_- \rangle) + \text{Re}(e^{-i\theta} \langle J_z J_+ \rangle)) + \frac{\cos^2 \xi}{4} \langle J_z^2 \rangle \\ &\quad - \sin^2 \xi \cos^2 \theta (\text{Re} \langle J_+ \rangle)^2 \end{aligned} \tag{C1}$$

and a table of first and second moments of the $\mathfrak{su}(2)$ elements $\{J_+, J_-, J_z\}$. Note that $\langle J_z \rangle_{e^{-itH_K|+}\rangle^{\otimes N}} = 0$.

1. $1 \leq K \leq \frac{N}{4}$

$$\begin{aligned}
& \text{Var}_{e^{-itH_K}|+}^{\otimes N} (\sin \xi \cos \theta J_x + \sin \xi \sin \theta J_y + \cos \xi J_z) = \\
& \frac{\sin^2 \xi}{2} \left(\frac{N+2}{2} + \frac{N+2}{4} (N+1-4K) \cos^{4K} t + \frac{N+2}{2} \frac{\cos^{2K} t - \cos^{4K} t}{\sin^2 t} + \frac{N+2}{2} \cot^2 t (1 - \cos^{2K} t) \right) \\
& + \frac{\sin^2 \xi \cos 2\theta}{2} \left(\frac{N+2}{4} (N+1-4K) \cos^{4K} t + \frac{N+2}{2} \cos^{4K} t \frac{\left(\frac{\cos 2t}{\cos^2 t}\right)^{K+1} - \frac{\cos 2t}{\cos^2 t}}{\frac{\cos 2t}{\cos^2 t} - 1} \right. \\
& \left. + \frac{N+2}{2} \frac{\cos^{2K} t \cos^{K-1} 2t \left(\left(\frac{\cos 2t}{\cos^2 t}\right)^K - 1\right)}{\frac{\cos 2t}{\cos^2 t} - 1} \right) \\
& + \frac{\sin 2\xi}{2} (N+2)K \sin t \sin \theta \cos^{2K-1} t + \frac{(N+2) \cos^2 \xi}{4} - \frac{\sin^2 \xi \cos^2 \theta (N+2)^2}{4} \cos^{4K} t \\
& = \frac{\sin^2 \xi}{2} \left(\frac{N+2}{2} - (1+4K) \cos^{4K} t + \frac{N+2}{2} \frac{\cos^{2K} t - \cos^{4K} t}{\sin^2 t} + \frac{N+2}{2} \cot^2 t (1 - \cos^{2K} t) \right) \\
& + \frac{\sin^2 \xi \cos 2\theta}{2} \left(-(1+4K) \cos^{4K} t + \frac{N+2}{2} \cos^{4K} t \frac{\left(\frac{\cos 2t}{\cos^2 t}\right)^{K+1} - \frac{\cos 2t}{\cos^2 t}}{\frac{\cos 2t}{\cos^2 t} - 1} \right. \\
& \left. + \frac{N+2}{2} \frac{\cos^{2K} t \cos^{K-1} 2t \left(\left(\frac{\cos 2t}{\cos^2 t}\right)^K - 1\right)}{\frac{\cos 2t}{\cos^2 t} - 1} \right) \\
& + \frac{\sin 2\xi}{2} (N+2)K \sin t \sin \theta \cos^{2K-1} t + \frac{(N+2) \cos^2 \xi}{4} \tag{C2}
\end{aligned}$$

2. $N/4 < K \leq \frac{N}{2}$

$$\begin{aligned}
& \text{Var}_{e^{-itH_K}|+}^{\otimes N} (\sin \xi \cos \theta J_x + \sin \xi \sin \theta J_y + \cos \xi J_z) = \frac{\sin^2 \xi}{2} \left(\frac{N+2}{2} \left(\frac{1 - \cos^{2(N+2-2K)} t}{\sin^2 t} \right) \right. \\
& \left. + \frac{(N+2)(3K-N-1)}{2} \cos^{2(N+1-2K)} t \right. \\
& \left. + \frac{N+2}{4} (N+1-2K) \cos^{2(N-2K)} t \right) \\
& + \frac{\sin^2 \xi \cos 2\theta}{2} \left(\frac{N+2}{2} \cos^{2K-1} 2t \frac{\left(\frac{\cos^2 t}{\cos 2t}\right)^{N+2-2K} - \frac{\cos^2 t}{\cos 2t}}{\frac{\cos^2 t}{\cos 2t} - 1} \right. \\
& \left. + \frac{(N+2)(3K-N-1)}{2} \cos^{2(N+1-2K)} t \cos^{4K-N-2} 2t \right. \\
& \left. + \frac{(N+2)(N+1-2K)}{4} \cos^{2(N-2K)} t \cos^{4K-N} 2t \right) \\
& + \frac{\sin 2\xi}{2} (N+2)K \sin t \sin \theta \cos^{2K-1} t + \frac{(N+2) \cos^2 \xi}{4} \\
& - \frac{\sin^2 \xi \cos^2 \theta (N+2)^2}{4} \cos^{4K} t \tag{C3}
\end{aligned}$$